AAPS PharmSciTech (2019) 20:98
DOI: 10.1208/s12249-019-1290-6

Research Article

Preparation and Characterization of Syringic Acid–Loaded TPGS Liposome with Enhanced Oral Bioavailability and *In Vivo* Antioxidant Efficiency

Yingkun Liu,[1] Congyong Sun,[1] Wenjing Li,[1] Michael Adu-Frimpong,[1] Qilong Wang,[1] Jiangnan Yu,[1,2,3] and Ximing Xu[1,2,3]

Received 23 October 2018; accepted 28 December 2018

Abstract. In this study, syringic acid–loaded TPGS liposome (SA-TPGS-Ls) was successfully prepared to improve oral bioavailability of syringic acid (SA). SA is a natural and notable antioxidant activity compound with its limited bioavailability ascribable to its poor aqueous solubility and fast elimination. Recently, TPGS has become a perfect molecular biomaterial in developing several carrier systems with sustained, controlled, and targeted the drug delivery. SA-TPGS-Ls was prepared *via* thin-film dispersion method and characterized in terms of particle size, stability, morphology, and encapsulation efficiency (EE). The results showed that SA-TPGS-Ls had regular spherical-shaped nanoparticles with EE of 96.48 ± 0.76%. The pharmacokinetic studies demonstrated a delayed MRT and prolonged $t_{1/2}$, while relative oral bioavailability increased by 2.8 times. Tissue distribution showed that SA-TPGS-Ls maintained liver drug concentration while delayed elimination was also observed in the kidney. In CCl_4-induced hepatotoxicity study, the activities of hepatic T-AOC, GSH-Px, CAT, GSH, and SOD were greatly elevated, while serum biological markers ALT, AST, and AKP were reduced after treatment of mice with SA-TPGS-Ls. Histopathological studies confirmed that SA-TPGS-Ls could remarkably improve the status of hepatic tissues. Collectively, SA-TPGS-Ls significantly improved the drug encapsulation efficiency, stability coupled with bioavailability of SA, hence increasing *in vivo* antioxidant activity of the drug.

KEY WORDS: syringic acid; vitamin E D-α-tocopheryl polyethylene glycol succinate; liposome; tissue distribution; antioxidant activity.

INTRODUCTION

Syringic acid (4-hydroxy-3, 5-dimethoxybenzoic acid, SA; Fig. 1) is a natural phenolic acid, which exists in many plants and foods, including walnut, black olive, cinnamon, and sesame (1). In clinical treatment, SA was used as a broad-spectrum antibiotic and strong antioxidant (2). Recent pharmacological studies demonstrated that SA possessed various activities, including anti-tumor (3), chemopreventive against skin cancer (4), and antithrombotic activity (5). Moreover, other findings demonstrated that SA has possesses free radical removal property culminating in prevention of oxidative stress in carbon tetrachloride (CCl_4)–induced liver damage (6). Nevertheless, the lipophilicity of SA coupled with the rapid excretion *in vivo* (7) results in low bioavailability and poor therapeutic effect.

Many nanoformulation techniques such as cyclodextrin inclusion compounds (8), liposomes (9), and micelles (10) have been reported to be ideal carriers for poorly soluble drugs. Liposomes, especially nanoliposomes modified with functional material, have become valuable promising carrier systems (11). More importantly, nanoliposomes modified with functional material might enhance the solubility and stabilization of entrapment agents, as well as alter tissue distribution and target drug to particular sites, while improving curative effects and reducing side effects (12).

D-Alpha tocopheryl polyethylene glycol 1000 succinate (TPGS, MW 1542 kDa) is a water-soluble ramification of natural vitamin E, synthesized through vitamin E succinate and polyethylene glycol (PEG) 1000 (13). Sanctioned by the US FDA (14) as a secure pharmaceutical aids, TPGS is regarded as a penetration accelerator, emulsifying agent, solutizer, additive, and stabilizer. It contained double advantages of both PEG and vitamin E in several drug delivery approaches, included prolonging of the drug half-time (15) as well as enhancing the amount of drug distributed to the cells. Various applications of TPGS in nanomedicines have been

[1] Center for Nano Drug/Gene Delivery and Tissue Engineering, School of Pharmacy, Jiangsu University, Zhenjiang, 212013, China.
[2] Department of Pharmaceutics, School of Pharmacy, Center for Nano Drug/Gene Delivery and Tissue Engineering, Jiangsu University, No.301, Xuefu Road, Jingkou District, Zhenjiang City, 212013, Jiangsu Province, China.
[3] To whom correspondence should be addressed. (e–mail: yjn@ujs.edu.cn; xmxu@ujs.edu.cn)

Published online: 04 February 2019

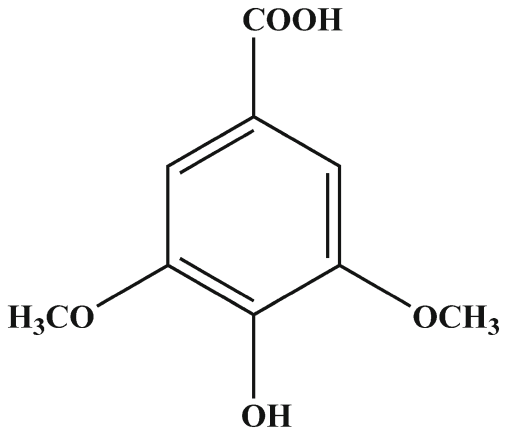

Fig. 1. Chemical structure of syringic acid

reported, namely solid self-nanodispersion (16), micelles (17), and liposomes based on TPGS, nanoparticles with TPGS-emulsified PLGA as well as TPGS-based copolymers. All these drug delivery systems can remarkably improve the solubility (18), penetrability, and stability (19) of the pharmaceutical preparation which can result in delaying, controlling, and targeting drug effects. Recently, TPGS has been employed as a modifier for liposomes in various studies. Exemplary, TPGS-loaded vesicle has been applied for oral administration of proteins and other drugs to improve limited oral bioavailability caused by gastrointestinal degradation and low pervasion (14).

Lately, nanoemulsions (20), cyclodextrin inclusion compounds (1), and liposomes (21) have been adopted as carriers to increase the solubility of SA. However, there was no nanoliposomes modified with functional material for enhancing oral bioavailability, and antioxidant effect of SA has been reported yet. In this study, syringic acid–loaded TPGS liposome (SA-TPGS-Ls) was successfully prepared, and the physicochemical properties were also characterized. The pharmacokinetics and tissue distribution studies of SA-TPGS-Ls were conducted, respectively. Moreover, *in vivo* antioxidant activity of SA and SA-TPGS-Ls was evaluated in CCl_4-induced hepatotoxic mice.

MATERIALS AND METHODS

Materials and Animals

Syringic acid (98% purity) was acquired from J&K Scientific Ltd. (Beijing, China). Vitamin E TPGS (98% purity) and lecithin from soybean (98% purity) were acquired from Aladdin Corporation (Shanghai, China). Castor oil, cholesterol, and carbon tetrachloride were purchased from Sinopharm Chemical Reagent Corporation (Shanghai, China). The biochemical test kits, *viz.*, malondialdehyde (MDA), superoxide dismutase (SOD), catalase (CAT), glutathione (GSH), total antioxidant capacity (T-AOC), glutathione peroxidase (GSH-Px), alanine aminotransferase (ALT), aspartate aminotransferase (AST), alkaline phosphatase (AKP), and Bradford protein were acquired from Jiancheng Bioengineering Institute (Nanjing, China). Millipore purifying system (Millipore Corporation, Bedford, MA, USA) was used to produce double-distilled water (DDW). Other substances involved were of analytical grade and commercially obtained.

Male Sprague Dawley rats (SD, 200 ± 20 g) and Kunming mice (KM, 20 ± 2 g) were acquired from the Center of Laboratory Animal Jiangsu University (Zhenjiang, China). The procedure for using the experimental animals in this study was followed in concordance with the protocol on animal experiments issued by the Jiangsu University Ethics Committee. All animals were acclimatized to the laboratory conditions for 3 days and were fasted for 12 h with free access to water prior to experiment.

Preparation of SA-TPGS-Ls

SA-TPGS-Ls was prepared by thin-film dispersion method based on previous studies (22). Ethanol (30 mL) was used as solvent to mix lecithin (720 mg), cholesterol (120 mg), and vitamin E TPGS (360 mg). The mixture was placed in a flask, followed by ultrasonic dissolution to yield a clear solution. Ethanol was removed with a rotary evaporator (Heidolph Co, Germany) under decompression at 45°C to obtain a thin film on the wall of the flask. Subsequently, ethanol (20 mL) containing SA (60 mg) was added to the complexes to form transparent solution. Then, the rotary evaporation was repeated at the same evaporation conditions to remove traces of ethanol. DDW (24 mL) was added to hydrate the solution at 45°C for 1 h. The mixed solution was homogenized with ultrasonic cell disruptor (Ningbo Scientz Biotechnology CO., LTD) for 10 min to obtain the small unilamellar vesicles (SUVS). Finally, 0.22 μm Millipore membrane was used to filter SUVS forming into SA-TPGS-Ls and preserved at 4°C for further study.

Characterization of SA-TPGS-Ls

Transmission Electron Microscopy

Transmission electron microscopy (TEM, Tecnai 12, FEI, Amsterdam, Holland) was employed to analyze the morphology of SA-TPGS-Ls. A drib of diluted SA-TPGS-Ls (2.5 mg/mL) with DDW (1:25, *v*/*v*) was dropped on a copper grid and stained with 2% phosphotungstic acid for 30 s. The sample was dried at a room temperature before TEM analysis.

Particle Size and Zeta Potential Analysis

Light-scattering instrument (Brookhaven 90 Plus PALS, Brookhaven Instruments Corp., Holtsville, NY, USA) was used to determine the physical attributes such as particle size, polydispersity index (PDI), and zeta potential of the SA-TPGS-Ls (2.5 mg/mL). After diluting the SA-TPGS-Ls (2.5 mg/mL) with DDW 1:1 into (3 mL), the sample was analyzed at 25°C and a scattering 90° angle. The measurements were carried out three times in triplicate.

Encapsulation Efficiency

The encapsulation efficiency (EE) of SA-TPGS-Ls was measured on the basis of existed studies (23). The non-encapsulated SA was filtered *via* cellulose nitrate membrane. The drug percentage of the encapsulated SA into SA-TPGS-

Ls was measured by separating free SA from SA-TPGS-Ls by filtering with 0.22 μm nitrocellulose membrane. The determination of SA content was calculated by reverse phase HPLC (Agilent 1260 liquid chromatography system, Agilent, San Jose, USA) equipped with a Nova-Pak C18 column (4.6 × 150 mm × 4 μm, Waters, Milford, MA, USA) set at 25°C with an ultraviolet detector with 272 nm. The mobile phase was methanol and acetic acid (0.05%) (30:70, *v*/*v*) at a flow rate of 1.0 mL/min. The validation of HPLC method was conducted according to ChP2015. Specifically, specificity, linearity, accuracy, and precision were validated. The determination of EE% of SA-TPGS-Ls was calculated though Eq. (1). All samples were performed in triplicates.

$$\mathrm{EE\%} = \left(1 - \frac{W_{\text{free SA}}}{W_{\text{total SA}}}\right) \times 100\% \quad (1)$$

Storage Stability

The storage stability of SA-TPGS-Ls was assessed on the account of variations in particle size and entrapment efficiency. Three newly prepared samples (5 mL) were stored at 4°C. At various periods (1, 7, 14, 21, and 28 days), the particle size and entrapment efficiency were determined, respectively.

Pharmacokinetic Studies

Animal Experiments

Six rats (200 ± 20 g) were randomized into two groups, SA group and SA-TPGS-Ls group with three mice in each group. The SA group rats were orally administered with SA (0.05% CMC-Na suspension, 25 mg/kg), while SA-TPGS-Ls group rats were administered with SA-TPGS-Ls (2.5 mg/mL) at the same dose. After oral administration, the blood samples (0.5 mL) were gathered from the rat orbital vein into heparinized tubes to obtain plasma at time points (8, 15, 25, 35, 45, 60, 75, 95, 120, 240, and 360 min), respectively. The blood sample was subsequently centrifuged for 10 min at 10,000 rpm to obtain plasma using Beckman coulter centrifuge.

Preparation of Samples and Determination

Plasma sample (200 μL) was add to methanol (500 μL) and 20 μL vanillin (internal standard, IS, 50 mg/mL) followed by vortex agitation for 2 min. Then, the mixtures were centrifuged at 10,000 rpm for 10 min and supernatant (15 μL) analyzed with HPLC. BAPP 2.3 pharmacokinetic software was applied to calculate pharmacokinetic parameters of the SA and SA-TPGS-Ls, such as the peak plasma concentration (C_{max}), mean residence time (MRT), time to attain peak concentration (T_{max}), and other associated indices. Experimental data was fitted to a non-compartment model to calculate the average of the pharmacokinetic parameters.

Tissue Distribution Studies

Animal Experiment

Twenty KM mice were used in the tissue distribution studies of free SA and SA-TPGS-Ls. Two groups of mice with each group consisting of ten mice were used for the study. The SA group mice were orally administrated with free SA (0.05% CMC-Na suspension, 50 mg/kg), while another group was provided the same quantity of SA-TPGS-Ls (2.5 mg/mL). The mice were sacrificed at different times (15, 30 min). Respective tissues were excised, washed, weighed, pretreated, and kept frozen at − 80°C until determination.

Treatment of Tissue Samples

Appropriate certain amount of normal saline (according to 1 mL/0.1 g) was added to tissue samples for homogenization. Then, 500 μL methanol and 20 μL of vanillin (internal standard, 50 mg/mL) were added to each of the homogenates (200 μL) followed by vortex agitation for 2 min. Then, obtained mixtures were centrifuged at 10,000 rpm for 10 min and the supernatant was (15 μL) analyzed with HPLC.

In vivo Antioxidant Activity

Animal Experiment

The *in vivo* antioxidant activity of SA and SA-TPGS-Ls was evaluated *via* hepatotoxicity induced by CCl_4 (23). Fifty KM mice were randomized in normal group (I), model group (II), positive group (III), SA group (IV), and SA-TPGS-Ls group (V). Groups I and II mice were orally administered with 0.05% CMC-Na (0.4 mL/20 g) consecutively for 7 days. Likewise, groups III and IV mice were given vitamin C and SA (50 mg/kg, suspended in 0.5% CMC-Na), respectively, while group V was given SA-TPGS-Ls (2.5 mg/mL, 50 mg/kg) for 7 days, respectively. Acute hepatic damage was induced experimentally on eighth day after pretreatment. Each of the mice was injected with CCl_4 in castor oil (0.2%, 10 mL/kg, *i.p.*), while group I was given equivalent quantity of only castor oil. After 24 h of CCl_4 intoxication, the mice were sacrificed through cervical dislocation after weighing. Blood samples (0.5 mL) were withdrawn from retro-orbital site and separated after clotting *via* centrifugation (3500 rpm, 10 min) to obtain the serum.

The fresh livers were dissected out and then washed weighed while partial liver (0.3 g) was placed in iced physiological saline (3.0 mL) for immediate homogenization using a Fluker homogenizer (Fluker, Germany). The supernatants obtained from the homogenate after centrifugation (3000 rpm, 10 min) were stored at − 80°C for further analysis. All the aforesaid procedures were carried out at 4°C.

Biochemical Assay

The activities of SOD, GSH-Px, GSH, T-AOC, MDA, and CAT in livers, as well as the ALT, AKP, and AST in serum, were assayed on the basis of the manufacturer's instructions. Protein quantity was ascertained using the Bradford test kits.

Histological Studies

Hematoxylin and eosin staining (H&E) could reflect directly of tissue lesions. In this present study, a small part of livers used for observation were excised then fixed in 4% neutral formaldehyde and were paraffin-embedded for pathological study. The sections were observed with an upright microscope (Eclipse Ni-U, Nikon, Japan) after staining sections with H&E. Photographs were captured at × 100 and × 200 magnifications, respectively.

Statistical Analysis

All the data were expressed as mean ± SD and analyzed using SPSS version 15.0. The statistical differences were evaluated by Student's *t* test and set at $p < 0.05$.

RESULTS AND DISCUSSION

Characterization of SA-TPGS-Ls

Particle Size, Zeta Potential, and Morphology of SA-TPGS-Ls

The TEM morphology of the prepared SA-TPGS-Ls revealed a homogeneous size, spherical shape, and small single-chamber structure (Fig. 2a). The average particle diameter of SA-TPGS-Ls was 40.01 ± 0.48 nm with an acceptable PDI of 0.22 ± 0.02, which were in agreement with the TEM results. The potential of SA-TPGS-Ls was − 38.50 ± 0.05 mv. It is generally agreed that the relatively high zeta potential (above 30 mv) indicated stable dispersion with resistance to agglomeration due to the electrostatic repulsion between similarly charged adjacent dispersed particles (24). The particle size distribution curves were unimodal (Fig. 2b). The low PDI indicated the uniformity of the liposomal particle size (25). Small particle size may be due to PEG1000; the polar part of TPGS could stretch out to the aqueous phase and shield the negatively charged liposomal surface leading to a thinner coating layer (14). As a part of the bilayer, TPGS participated in the formation of TPGS-SA-Ls by altering the geometric packing and thus the diameter of TPGS-SA-Ls. Therefore, these results indicated that SA-TPGS-Ls monodispersed stable system and high absolute zeta potential could maintain homogeneity of particle sizes. Moreover, small particle size could avoid the ingestion by the reticuloendothelial system, culminating in increasing drug accumulation in particular tissues with direct influence on *in vivo* circulating time and distribution (9). All these parameters indicate that SA-TPGS-Ls might increase the solubility of SA and thus enhance the absorption of SA *in vivo*.

Encapsulation Efficiency of SA-TPGS-Ls

The determination of SA content was calculated by standard curve $Y = 52.213X - 110.64$ ($n = 5$, $r^2 = 0.9993$), and linearly ranged in 5–100 μg/mL, where X is the concentration of SA in SA-TPGS-Ls and Y is the peak area of SA. The encapsulation efficiency (EE) of SA-TPGS-Ls was estimated as 96.48 ± 0.76%. The EE is one of the most vital indicators for evaluating the quality of liposomes and a major cause for the therapeutic effect. The EE of SA-TPGS-Ls achieved was 96.48 ± 0.76%, which was higher than the previous study (21). It has been shown previously that TPGS could efficiently emulsified lipophilic drugs during nanoparticle fabrication leading to high EE of drugs (14). In comparison with the conventional emulsifier polyvinyl alcohol, TPGS showed higher emulsification efficiency (26). TPGS as an active matrix component could enhanced the hydrophobic interaction between lipophilic vitamin E part of TPGS and hydrophobic SA thus resulting in higher EE% (27). Hence, TPGS could be considered as surfactant or a part of liposomal formulation, resulting in maximum SA encapsulation efficiency (28).

Storage Stability of SA-TPGS-Ls

During the storage period of SA-TPGS-Ls, no changes in appearance, layer separations, and original color were observed in the liposomal formulation (Fig. 2c). Table I showed the average particle diameter (43.00 ± 1.67) and encapsulation efficiency (95.00 ± 0.77) of the SA-TPGS-Ls during the storage period (28 days) at 4°C. It is worth noting that the average particle diameter slight increase (within the

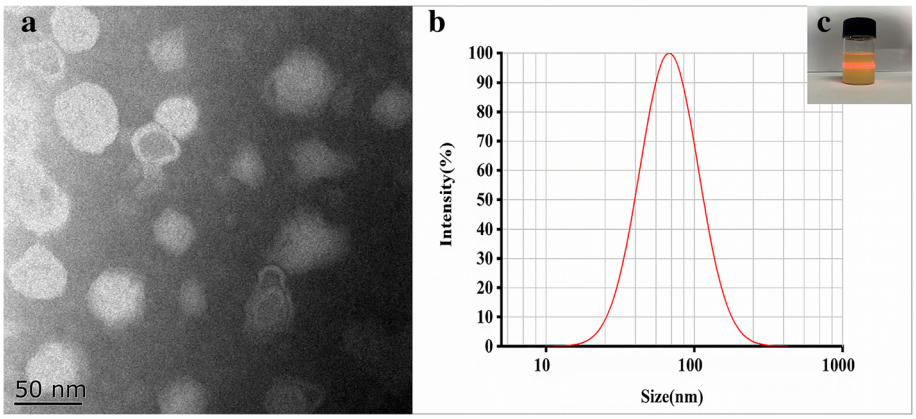

Fig. 2. TEM image of SA-TPGS-Ls (**a**), particle size distribution of SA-TPGS-Ls (**b**), and the appearance evaluation of SA-TPGS-Ls (**c**)

range of 10 nm) in particle size and EE decreased slightly (not more than 3%). The aggregation, fusion, or sedimentation of the liposomes could easily occur during storage process (29). SA-TPGS-Ls surface was negatively charged due to the presence of phospholipids, which would maintain the stability of the liposome solution through electrostatic repulsion (12). Furthermore, when TPGS was employed as the matrix material, no such aforementioned instability phenomenon occurred. It may be owing to the special physicochemical characteristics of TPGS. The amphiphile structure of surfactants aids them to align at the outer surfaces of liposomal droplets (30). Consequently, this results in stability promotion through free energy lowering at the boundary between organic and aqueous phases which leads to resistance to liposomal flocculation and aggregation (22). The presence of long-chain PEG in the surfaces of TPGS-based liposomes could enhance further the vesicular stability *via* steric hindrance (31). Therefore, the stability of SA-TPGS-Ls was acceptable which suggested that the liposomal bilayer was an appropriate carrier for SA.

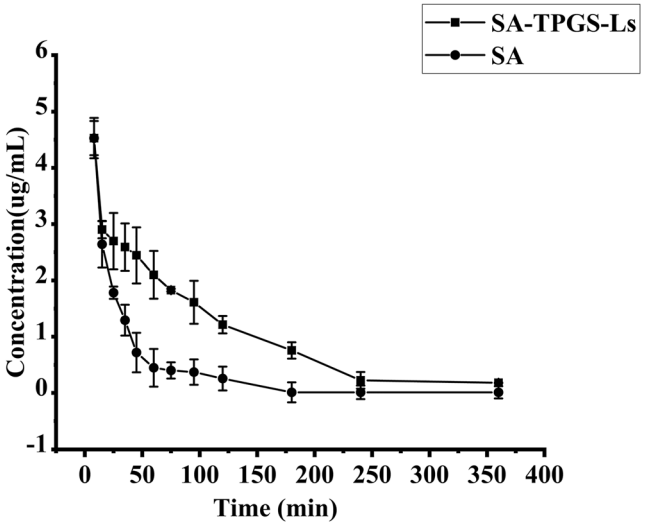

Fig. 3. Mean plasma concentration-time curve of free SA and SA-TPGS-Ls after single oral administration in rats (mean ± SD, 25 mg/kg, $n = 3$)

Pharmacokinetic Studies of SA-TPGS-Ls

The plasma of SA content was calculated by standard curve $Y = 5.9543X + 0.0648$ ($r^2 = 0.9996$), and linearly ranged in 0.125–8 μg/mL, where X is the concentration of SA in plasma and Y is the peak area ratios of SA to internal standard. As shown in Fig. 3 and Table II, SA reached C_{max} attained rapidly at 8 min and eliminated from rat plasma rapidly after the oral administration of free SA and SA-TPGS-Ls which were in accordance with previous work (21). However, compared with free SA, the SA-TPGS-Ls had delayed $t_{1/2}$ (50.03 ± 15.29 *vs* 17.67 ± 0.93, $p < 0.05$) and prolonged MRT (82.76 ± 2.66 *vs* 39.30 ± 1.01, $p < 0.001$), respectively. A prolonged $t_{1/2}$ of SA-TPGS-Ls within a certain range could have some pharmaceutical significance (34). Liposomes have been suggested to relatively prolong MRT while delaying $t_{1/2}$ which explains their sustained release attributes (32). Additionally, surface modification of the liposomes with TPGS could protect the drug from decomposition of enzyme and immune system because the main part of the drug moiety remains in the liposome vesicles (14). In addition, SA-TPGS-Ls increased $AUC_{0-360min}$ (338.08 ± 3.65) by 2.8-fold compared to the unformulated SA and maintained the plasma SA concentration higher than the unformulated SA even at 6-h post-dose.

These results demonstrated that SA-TPGS-Ls enhanced *in vivo* retention time of SA after oral administration. Small particle size (less than 100 nm) promoted full and stable gastrointestinal absorption by expanding the superficial area of preparations (33). Besides, the high EE of drug formulation indicates that more SA was encapsulated in liposomes, thus preventing the direct contact between drugs and esophagus. TPGS can also stabilize liposomes probably through prevention of their degradation by the pancreatic enzymes *via* steric hindrance caused by the PEG chain. Thus, the drug exposure time was prolonged by SA-TPGS-Ls which might ensure sustained release of SA which could increase circulation time thereby minimizing frequent administration of the drug (33). Liposome phospholipid bilayers could enhance the membrane permeability and cellular absorption. Furthermore, when a permeation enhancer TPGS was added to preparation, it improved its permeation through the skin or intestinal walls (22). Through oral delivery, TPGS-based liposomes might improve limited oral bioavailability of SA which was caused by gastrointestinal degradation and low pervasion (34). Collectively, the SA-TPGS-Ls is a novel approach of improving the oral bioavailability of SA.

Tissue Distribution Studies of SA-TPGS-Ls

Standard curves and linear ranges for SA determination in each tissue (heart, liver spleen, lung, kidney, and brain) were built as shown in Table III. The distribution of SA in the tissues was evaluated through the aforementioned standard curves. The concentration of SA in each tissue of mice at several time points was later shown in Fig. 4. During 15 min after dosing, it was found that SA was quickly and widely distributed in the systemic circulation but accumulated more in the kidney, followed by the liver and slightly in other organs (*viz.*, heart, spleen, lung, and brain). The same trend

Table I. Storage Stability of SA-TPGS-Ls ($n = 3$)

Time (day)	1	7	14	21	28
Particle size	40.01 ± 0.48	40.33 ± 0.87	41.39 ± 1.21	42.34 ± 1.54	43.00 ± 1.67
PDI	0.22 ± 0.02	0.23 ± 0.03	0.31 ± 0.03	0.31 ± 0.03	0.32 ± 0.03
EE (%)	96.48 ± 0.76	96.00 ± 0.58	95.98 ± 0.39	95.90 ± 0.55	95.00 ± 0.77

PDI, polydispersity index; *EE*, encapsulation efficiency

Table II. The *In Vivo* Pharmacokinetic Parameters of Free SA and SA-TPGS-Ls After Single Oral Administration in Rats (Mean ± SD, 25 mg/kg, $n = 3$)

Parameters	SA-TPGS-Ls	SA
C_{max} (g/mL)	4.50 ± 0.04	4.50 ± 0.04
T_{max} (min)	8.00	8.00
MRT (min)	82.76 ± 2.66***	39.30 ± 1.01
$T_{1/2}$ (min)	50.03 ± 15.29*	17.67 ± 0.93
$AUC_{0–360}$ (g min/mL)	338.08 ± 3.65***	120.58 ± 2.92

MRT, mean residence time; *SA-TPGS-Ls*, syringic acid–loaded TPGS liposome; *SA*, syringic acid
*Values are significantly different from the SA group at the level of $p < 0.05$. *** Values are significantly different from the SA group at the level of $p < 0.001$

was observed after the oral administration of both the free SA and SA-TPGS-Ls. The SA accumulation pattern in the liver (Fig. 4) agreed with the previous study (21) which suggested that the accumulation of SA in the liver was due to passive trapping (35).

SA gradually reduced in tissues after oral administration of SA and SA-TPGS-Ls within 30-min period. In SA-TPGS-Ls group, the drug concentration demonstrated delayed elimination which was also observed in the liver and kidney. This indicated that SA-TPGS-Ls was a monodispersed stabilization system that could effectively enhance the accumulation of drugs in the liver (36). This may be due to nanoliposomes that usually deliver drugs selectively to the target sites thereby maintaining high drug concentrations in systemic circulation (37). These findings indicated that TPGS might play a crucial role in the SA absorption for the enhanced antioxidant activity.

In vivo Antioxidant Activity of SA-TPGS-Ls

Effect of SA-TPGS-Ls on Relative Organ Weights

The liver weight coefficient (%) of mice in each group is presented in Table IV. There was an obvious increase in the liver weight coefficient for the model group comparing with the normal group ($p < 0.001$). These results suggested that CCl_4 was able to induce liver hepatocellular injury and hypertrophy, which result in increasing the mice liver weight. Contrariwise, mice in the groups (VC, SA, and SA-TPGS-Ls) pretreated for 7 days slightly increased liver weight coefficient than in the normal group ($p <$

Table III. Linear Ranges, Standard Curves, and Regression Coefficients of SA in Different Biosamples ($n = 3$)

Biosamples	Linear range (μg/mL)	Calibration curves	r^2
Heart	0.05–1	$Y = 0.1248X + 0.0200$	0.9958
Liver	0.125–4	$Y = 0.6667X + 0.0151$	0.9938
Spleen	0.05–1	$Y = 0.7426X - 0.0596$	0.9948
Lung	0.05–1	$Y = 0.6885X + 0.0049$	0.9984
Kidney	0.125–8	$Y = 0.8018X + 0.0406$	0.9926
Brain	0.05–1	$Y = 0.6953X + 0.0270$	0.9938

Table IV. Effects of SA and SA-TPGS-Ls on the Activities of GSH-Px, GSH, T-SOD, T-AOC, MDA, and CAT in Livers and Levels of ALT, AST, and AKP in serum

Group	Serum			Liver weight coefficient (%)	Liver					
	ALT (U/L)	AST (U/L)	AKP (U/L)		$GSH\text{-}P_X$ (U/mL)	SOD (U/mL)	CAT (U/mL)	GSH (U/mL)	MDA (nmol/mL)	T-AOC ($\times 10^{-2}$U/mL)
I	19.90 ± 3.90	87.14 ± 49.02	24.04 ± 7.60	4.05 ± 0.26	437.74 ± 22.41	121.34 ± 9.69	32.48 ± 12.1	14.65 ± 8.19	1.50 ± 0.32	0.88 ± 0.20
II	12,592.60 ± 1332.40***	1403.40 ± 282.42***	35.46 ± 7.33**	5.06 ± 0.30***	337.53 ± 43.47**	115.82 ± 6.67**	21.22 ± 6.7**	3.18 ± 0.68***	1.89 ± 0.35	0.14 ± 0.16***
III	4666.20 ± 2993.40###	576.51 ± 317.47###	14.07 ± 3.42###	4.49 ± 0.32*	436.03 ± 30.70###	126.05 ± 26.89###	26.90 ± 3.40###	24.92 ± 6.19###	1.65 ± 0.22	0.37 ± 0.36#
IV	7639.30 ± 3934.00###	901.67 ± 433.27###	14.00 ± 3.75###	4.66 ± 0.48*	396.19 ± 48.05###	115.52 ± 18.19	26.10 ± 3.90###	19.96 ± 9.91###	1.48 ± 0.38	0.33 ± 0.18
V	4081.80 ± 2476.40###	507.13 ± 244.47###	11.50 ± 2.96###	4.59 ± 0.49*	407.57 ± 15.94###	120.38 ± 21.98	41.60 ± 12.50###	20.58 ± 8.04###	1.40 ± 0.38	0.44 ± 0.42

ALT, alanine aminotransferase; *AST*, aspartate aminotransferase; *AKP*, alkaline phosphatase; *GSH-P_X*, glutathione peroxidase; *SOD*, superoxide dismutase; *CAT*, catalase; *GSH*, glutathione; *MDA*, malondialdehyde; *T-AOC*, total antioxidant capacity
Groups I, II and III represent the groups of normal control, model control, and positive control, respectively. Group IV was treated with 50 mg/kg of free SA, and group V was treated with 50 mg/kg of SA-TPGS-Ls
Each value is presented as mean ± SD ($n = 6$). *Values are significantly different from the normal group at the level of $p < 0.05$. **Values are significantly different from the normal group at the level of $p < 0.01$. ***Values are significantly different from the normal group at the level of $p < 0.001$
Values are significantly different from the model group at the level of $p < 0.05$. ## *Values are significantly different from the model group at the level of $p < 0.01$.* ### *Values are significantly different from the model group at the level of $p < 0.001$*

0.05) as well as improved liver hepatocellular injury and hypertrophy. These demonstrated that SA and SA-TPGS-Ls could reduce the increased liver weight caused by CCl_4.

Effect of SA-TPGS-Ls on the Activities of Serums ALT, AST, and AKP

CCl_4 is a prototype of hepatotoxin used usually in experimental models for causing oxidative stress-associated liver injury (38). The activity enhancement of serums ALT, AST, and AKP is commonly used as the diagnostic index for the damage of hepatocytes. Under abnormal circumstances, this damage to hepatocellular membrane caused by free radical–induced lipid peroxidation leads to leakage of the intracellular hepatic enzymes (39). Accordingly, this is manifested by marked elevation in levels of the serums ALT ($p < 0.001$), AST ($p < 0.001$), and AKP ($p < 0.01$) in the model group compared to the normal group (Table IV). This demonstrated that CCl_4 could cause serious damage to hepatocytes. After administration of SA and SA-TPGS-Ls for 7 days at a dose of 50 mg/kg, the ALT, AST, and AKP levels were markedly lowered ($p < 0.001$) compared to the model group. These findings were further confirmed by histopathology. The aforementioned results further suggested that SA especially SA-TPGS-Ls had anti-hepatotoxic activity against CCl_4-induced acute mice liver injury.

Effect of SA-TPGS-Ls of Hepatic Antioxidant Enzymes Activities

CCl_4-induced liver damage is due to its capability to inhibit antioxidant enzyme (40). In this regard, CCl_4 is metabolized *via* cytochrome P-450-mediated electron transfer to the C–Cl bond, which forms trichloromethyl radical (-CCl_3·). This radical further metabolized to the reactive intermediate trichloromethylperoxyl radicals (CCl_3OOC·) intermediate which is more reactive (41). These free radicals cause severe intracellular injury by donating their electron to the organic components in the hepatocytes thereby oxidizing them. However, enzymes like SOD, CAT, and GSH-Px are principal antioxidant defense system which could achieve cell protective effects and their extracellular matrix against oxidative damage by scavenging free radicals (42). As an intracellular compound, SOD can improve oxidative damage which is initiated by superoxide anion (43). The main biological function of GSH-Px and CAT is to remove lipid peroxides and H_2O_2.

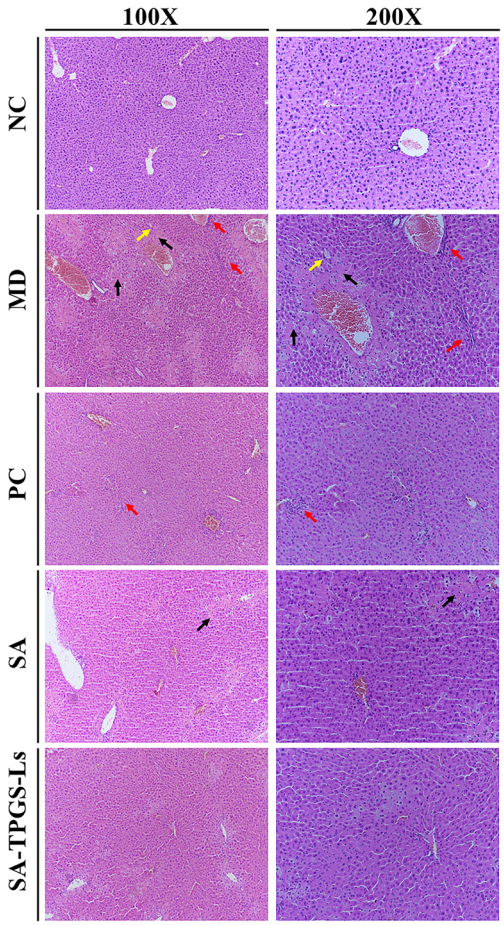

Fig.5. H & E stain. Effects of SA and SA-TPGS-Ls on histopathology of liver in mice NC, normal group; MD, model group; PC, positive group (VC, 50 mg/kg); SA, free SA group (50 mg/kg); SA-TPGS-Ls, SA-TPGS-Ls group (50 mg/kg). Black arrow: centrilobular necrosis and loss of cellular boundaries with disruption of membranes; red arrow: inflammatory cell infiltration; yellow arrow: liver cellular hypertrophy

Table IV showed that the activities of CAT ($p < 0.01$), GSH-P_X ($p < 0.01$), and SOD ($p < 0.01$) were significantly lowered in model group than in normal group after CCl_4 treatment. Oral administration of VC remarkably ameliorated the elevated enzyme levels in CCl_4-induced mice close to the normal. The administration of SA and SA-TPGS-Ls by dosage of 50 mg/kg daily for 7 days

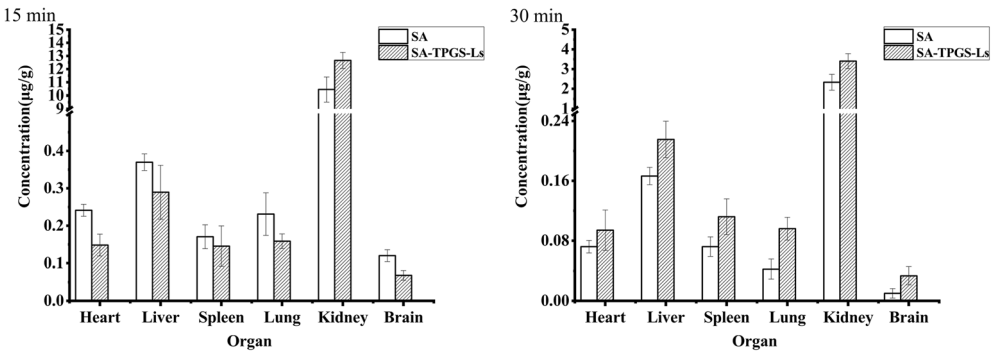

Fig. 4. Distribution profile of SA in mice tissues at 15 min and 30 min after oral administration of SA and SA-TPGS-Ls. The freshly prepared SA and SA-TPGS-Ls were administered at dose of 50 mg/kg. Values presented represent mean ± SD, $n = 5$

markedly improved the activities of these antioxidant enzymes in varying degrees. Specifically, the activity of GSH-P_X and CAT were statistically increased ($p < 0.001$), while the SOD activity was increased but did not reach statistical significance level ($p > 0.05$) compared with the model group. These results were analogous to the liver-protective effects described in chlorogenic acid and its liposomal formulation, under similar condition (23). Administration of SA/SA-TPGS-Ls along with CCl_4 removed the toxic reactive radicals of CCl_4 thereby increasing synthesis of endogenous antioxidant system, and this conferred enhanced protection against oxidative injuries. This accordingly increased levels of the hepatic CAT, SOD, and GSH-PX. It is worth noting that SA-TPGS-Ls successfully prevented CCl_4 damage and maintained enzyme activity close to normal levels. These results further support our finding that SA especially SA-TPGS-Ls attenuates hepatic injury in CCl_4-treated mice.

Effect of SA-TPGS-Ls on the Non-enzymatic System

For the end-product of lipid peroxidation to cellular and cell membrane damage, MDA is a frequently used biochemical marker for antioxidant activity evaluation *in vivo* (44). The MDA production was raised in the CCl_4 injury model group as shown in Table IV. In contrast, supplementation of SA (50 mg/kg) and SA-TPGS-Ls (50 mg/kg) effectively inhibited the MDA generation ($p > 0.05$) when compared with the model group. Furthermore, the hepatic MDA level of SA-TPGS-Ls group was lower than the SA group. Therefore, the SA-TPGS-Ls could ameliorate generation of MDA *via* its antioxidant effect. GSH is a non-enzymatic antioxidant which is oxidized to GSSH by GSH-Px and then GSSH is reduced back to GSH by GSR (39). The heightened oxidative stress caused by CCl_4 results in decrease in GSH contents coupled with declined GSH-Px activity in the liver. Pretreatment with SA and SA-TPGS-Ls greatly ($p < 0.001$) elevated GSH toward the normal level compared with the model group (Table IV). Similarly, T-AOC also reflects the ability of the non-enzymatic antioxidant defense system (45). The results showed that SA and SA-TPGS-Ls pretreatments could increase T-AOC level in the livers which suggested that non-enzymatic system was enhanced particularly by SA supplementation.

In summary, the increase in GSH and T-AOC, as well as the decrease in MDA level, could evaluate antioxidant activity of SA and SA-TPGS-Ls. The SA-TPGS-Ls possess the antioxidant effect as well as the hepatoprotective property *via* protecting hepatocytes against oxidative stress, while the nanoformulation of SA *via* liposomes also further enhanced its antioxidant effects (46).

Effect of SA-TPGS-Ls on the Histopathological Examination

Liver histology also showed convincing evidence. Stained section (Fig. 5) indicated that liver sections of the normal group contained well-preserved cytoplasm, prominent nuclei, and the clearly visible central vein. Injection of CCl_4 markedly caused large areas of centrilobular necrosis and loss of cellular boundaries with disruption of membranes (black arrow) with total loss of hepatic architecture with the cellular hypertrophy (yellow arrow) and inflammatory cell infiltration (red arrow) in the livers (47). This reasonably explains the disorder of liver enzymes in the model group mice. However, mice pretreated with VC (50 mg/kg) and SA (50 mg/kg) substantially improved the damage induced by CCl_4 compared with the model group. Only small areas of necrosis or inflammatory cell infiltration were observed in the liver slice of VC and SA groups. In addition, the SA-TPGS-Ls-treated mice demonstrated no obvious necrosis with almost intact liver structure. This effect could be attributed to the TPGS that enhanced antioxidant activity of SA, thus attenuating the CCl_4-associated oxidative stress and restored normal physiological liver functions.

CONCLUSIONS

In this study, a novel SA-TPGS-Ls was successfully prepared. The SA-TPGS-Ls has notable attributes, such as homogeneous size and high encapsulation efficiency and stability. The pharmacokinetic and tissue distribution studies proved the higher bioavailability and liver accumulation of SA-TPGS-Ls. The *in vivo* antioxidant activity confirmed the high oral bioavailability can enhance therapeutic effect of SA. The enhanced antioxidant effects of SA-TPGS-Ls were revealed by the improvement of the activities of antioxidant enzymatic/non-enzymatic systems and reduction of lipid peroxidation in the liver. Therefore, the TPGS could act as an ideal carrier material for SA to increase *in vivo* antioxidant activities.

FUNDING INFORMATION

This work was supported by the National Natural Science Foundation of China (Grants 81720108030 and 81773695), National "Twelfth Five-Year" Plan for Science and Technology Support (Grant 2013BAD16B07-1).

COMPLIANCE WITH ETHICAL STANDARDS

The procedure for using the experimental animals in this study was followed in concordance with the protocol on animal experiments issued by the Jiangsu University Ethics Committee.

Conflict of Interests The authors declare that they have no conflict of interest.

REFERENCES

1. Song LX, Wang HM, Xu P, Yang Y, Zhang ZQ. Experimental and theoretical studies on the inclusion complexation of syringic acid with alpha-, beta-, gamma- and heptakis(2,6-di-O-methyl)-beta-cyclodextrin. Chem Pharm Bull. 2008;56(4):468–74. https://doi.org/10.1248/cpb.56.468.
2. Haneef J, Chadha R. Antioxidant-based eutectics of irbesartan: viable multicomponent forms for the management of hypertension. AAPS PharmSciTech. 2018;19(3):1191–204. https://doi.org/10.1208/s12249-017-0930-y.
3. Kampa M, Alexaki VI, Notas G, Nifli AP, Nistikaki A, Hatzoglou A, et al. Antiproliferative and apoptotic effects of selective phenolic acids on T47D human breast cancer cells:

potential mechanisms of action. Breast Cancer Res. 2004;6(2):R63–74. https://doi.org/10.1186/bcr752.
4. Ha SJ, Lee J, Park J, Kim YH, Lee NH, Kim YE, et al. Syringic acid prevents skin carcinogenesis via regulation of NoX and EGFR signaling. Biochem Pharmacol. 2018;154:435–45. https://doi.org/10.1016/j.bcp.2018.06.007.
5. Choi J-H, Kim S. Mechanisms of attenuation of clot formation and acute thromboembolism by syringic acid in mice. J Funct Foods. 2018;43:112–22. https://doi.org/10.1016/j.jff.2018.02.004.
6. Itoh A, Isoda K, Kondoh M, Kawase M, Watari A, Kobayashi M, et al. Hepatoprotective effect of syringic acid and vanillic acid on CCl_4-induced liver injury. Biol Pharm Bull. 2010;33(6):983–7. https://doi.org/10.1248/bpb.33.983.
7. Zhou W, Zhang Y, Ning S, Li Y, Ye M, Yu Y, et al. Automated on-line SPE/multi-stage column-switching and benzoic acid-based QAMS/RODWs-HPLC for oral pharmacokinetics of syringic acid and salicylic acid in rats. Chromatographia. 2012;75(15–16):883–92. https://doi.org/10.1007/s10337-012-2270-0.
8. Kfoury M, Sahraoui AL-H, Bourdon N, Laruelle F, Fontaine J, Auezova L, et al. Solubility, photostability and antifungal activity of phenylpropanoids encapsulated in cyclodextrins. Food Chem. 2016;196:518–25. https://doi.org/10.1016/j.foodchem.2015.09.078.
9. Zhu Y, Wang M, Zhang J, Peng W, Firempong CK, Deng W, et al. Improved oral bioavailability of capsaicin via liposomal nanoformulation: preparation, in vitro drug release and pharmacokinetics in rats. Arch Pharm Res. 2015;38(4):512–21. https://doi.org/10.1007/s12272-014-0481-7.
10. J-n Y, Zhu Y, Wang L, Peng M, S-s T, Cao X, et al. Enhancement of oral bioavailability of the poorly water-soluble drug silybin by sodium cholate/phospholipid-mixed micelles. Acta Pharmacol Sin. 2010;31(6):759–64. https://doi.org/10.1038/aps.2010.55.
11. Chu C, S-s T, Xu Y, Wang L, Fu M, Ge Y-r, et al. Proliposomes for oral delivery of dehydrosilymarin: preparation and evaluation in vitro and in vivo. Acta Pharmacol Sin. 2011;32(7):973–80. https://doi.org/10.1038/aps.2011.25.
12. Li J, Cheng X, Chen Y, He W, Ni L, Xiong P, et al. Vitamin E TPGS modified liposomes enhance cellular uptake and targeted delivery of luteolin: an in vivo/in vitro evaluation. Int J Pharm. 2016;512(1):262–72. https://doi.org/10.1016/j.ijpharm.2016.08.037.
13. Lamm MS, DiNunzio J, Khawaja NN, Crocker LS, Pecora A. Assessing mixing quality of a copovidone-TPGS hot melt extrusion process with atomic force microscopy and differential scanning calorimetry. AAPS PharmSciTech. 2016;17(1):89–98. https://doi.org/10.1208/s12249-015-0387-9.
14. Zhang Z, Tan S, Feng S-S. Vitamin E TPGS as a molecular biomaterial for drug delivery. Biomaterials. 2012;33(19):4889–906. https://doi.org/10.1016/j.biomaterials.2012.03.046.
15. Mi Y, Zhao J, Feng S-S. Vitamin E TPGS prodrug micelles for hydrophilic drug delivery with neuroprotective effects. Int J Pharm. 2012;438(1–2):98–106. https://doi.org/10.1016/j.ijpharm.2012.08.038.
16. Xu JN, Ma YQ, Xie YB, Chen YC, Liu Y, Yue PF, et al. Design and evaluation of novel solid self-nanodispersion delivery system for andrographolide. AAPS PharmSciTech. 2017;18(5):1572–84. https://doi.org/10.1208/s12249-016-0627-7.
17. Cholkar K, Gunda S, Earla R, Pal D, Mitra AK. Nanomicellar topical aqueous drop formulation of rapamycin for back-of-the-eye delivery. AAPS PharmSciTech. 2015;16(3):610–22. https://doi.org/10.1208/s12249-014-0244-2.
18. Srivalli KMR, Mishra B. Improved aqueous solubility and antihypercholesterolemic activity of ezetimibe on formulating with hydroxypropyl-beta-cyclodextrin and hydrophilic auxiliary substances. AAPS PharmSciTech. 2016;17(2):272–83. https://doi.org/10.1208/s12249-015-0344-7.
19. Yang CL, Wu TT, Qi Y, Zhang ZP. Recent advances in the application of vitamin E TPGS for drug delivery. Theranostics. 2018;8(2):464–85. https://doi.org/10.7150/thno.22711.
20. Polychniatou V, Tzia C. Evaluation of surface-active and antioxidant effect of olive oil endogenous compounds on the stabilization of water-in-olive-oil nanoemulsions. Food Chem. 2018;240:1146–53. https://doi.org/10.1016/j.foodchem.2017.08.044.
21. Sun C, Yuan Y, Omari-Siaw E, Tong S, Zhu Y, Wang Q, et al. An efficient HPLC method for determination of syringic acid liposome in rats plasma and mice tissue: pharmacokinetic and biodistribution application. Curr Pharm Anal. 2018;14(1):41–52. https://doi.org/10.2174/1573412912666160926101220.
22. Mu L, Feng SS. A novel controlled release formulation for the anticancer drug paclitaxel (Taxol (R)): PLGA nanoparticles containing vitamin E TPGS. J Control Release. 2003;86(1):33–48. https://doi.org/10.1016/s0168-3659(02)00320-6.
23. Feng Y, Sun C, Yuan Y, Zhu Y, Wan J, Firempong CK, et al. Enhanced oral bioavailability and in vivo antioxidant activity of chlorogenic acid via liposomal formulation. Int J Pharm. 2016;501(1–2):342–9. https://doi.org/10.1016/j.ijpharm.2016.01.081.
24. Omari-Siaw E, Wang Q, Sun C, Gu Z, Zhu Y, Cao X, et al. Tissue distribution and enhanced in vivo anti-hyperlipidemic-antioxidant effects of perillaldehyde-loaded liposomal nanoformulation against Poloxamer 407-induced hyperlipidemia. Int J Pharm. 2016;513(1–2):68–77. https://doi.org/10.1016/j.ijpharm.2016.08.042.
25. Zhu Y, Wang M, Zhang Y, Zeng J, Omari-Siaw E, Yu J, et al. In vitro release and bioavailability of silybin from micelle-templated porous calcium phosphate microparticles. AAPS PharmSciTech. 2016;17(5):1232–9. https://doi.org/10.1208/s12249-015-0460-4.
26. Turk CTS, Oz UC, Serim TM, Hascicek C. Formulation and optimization of nonionic surfactants emulsified nimesulide-loaded PLGA-based nanoparticles by design of experiments. AAPS PharmSciTech. 2014;15(1):161–76. https://doi.org/10.1208/s12249-013-0048-9.
27. Zhang MY, He JH, Zhang WL, Liu JP. Fabrication of TPGS-stabilized liposome-PLGA hybrid nanoparticle via a new modified nanoprecipitation approach: in vitro and in vivo evaluation. Pharm Res. 2018;35(11):13. https://doi.org/10.1007/s11095-018-2485-3.
28. Suksiriworapong J, Rungvimolsin T, A-gomol A, Junyaprasert VB, Chantasart D. Development and characterization of lyophilized diazepam-loaded polymeric micelles. AAPS PharmSciTech. 2014;15(1):52–64. https://doi.org/10.1208/s12249-013-0032-4.
29. Malekar SA, Sarode AL, Bachii AC, Worthen DR. The localization of phenolic compounds in liposomal bilayers and their effects on surface characteristics and colloidal stability. AAPS PharmSciTech. 2016;17(6):1468–76. https://doi.org/10.1208/s12249-016-0483-5.
30. Vicentini F, Casagrande R, Verri WA, Georgetti SR, Bentley M, Fonseca MJV. Quercetin in lyotropic liquid crystalline formulations: physical, chemical and functional stability. AAPS PharmSciTech. 2008;9(2):591–6. https://doi.org/10.1208/s12249-008-9091-3.
31. Shao Y, Yang L, Han H-K. TPGS-chitosome as an effective oral delivery system for improving the bioavailability of coenzyme Q10. Eur J Pharm Biopharm. 2015;89:339–46. https://doi.org/10.1016/j.ejpb.2014.12.026.
32. Yi C, Fu M, Cao X, Tong S, Zheng Q, Firempong CK, et al. Enhanced Oral bioavailability and tissue distribution of a new potential anticancer agent, Flammulina velutipes sterols, through liposomal encapsulation. J Agric Food Chem. 2013;61(25):5961–71. https://doi.org/10.1021/jf3055278.
33. Wei Q, Yang Q, Wang Q, Sun C, Zhu Y, Niu Y, et al. Formulation, characterization, and pharmacokinetic studies of 6-gingerol-loaded nanostructured lipid carriers. AAPS PharmSciTech. 2018;19(8):3661–9. https://doi.org/10.1208/s12249-018-1165-2.
34. Li QR, Zhan SY, Liu Q, Su H, Dai X, Wang H, et al. Preparation of a sustained-release nebulized aerosol of R-terbutaline hydrochloride liposome and evaluation of its anti-asthmatic effects via pulmonary delivery in guinea pigs. AAPS PharmSciTech. 2018;19(1):232–41. https://doi.org/10.1208/s12249-017-0816-z.
35. Xu X, Capito RM, Spector M. Plasmid size influences chitosan nanoparticle mediated gene transfer to chondrocytes. J Biomed Mater Res A. 2008;84A(4):1038–48. https://doi.org/10.1002/jbm.a.31479.

36. Wang Y, Wang S, Firempong CK, Zhang H, Wang M, Zhang Y, et al. Enhanced solubility and bioavailability of naringenin via liposomal nanoformulation: preparation and in vitro and in vivo evaluations. AAPS PharmSciTech. 2017;18(3):586–94. https://doi.org/10.1208/s12249-016-0537-8.
37. Li K, Wang SJ. Preparation, pharmacokinetic profile, and tissue distribution studies of a liposome-based formulation of SN-38 using an UPLC-MS/MS method. AAPS PharmSciTech. 2016;17(6):1450–6. https://doi.org/10.1208/s12249-016-0484-4.
38. Bhattacharyya S, Ahammed SM, Saha BP, Mukherjee PK. The gallic acid-phospholipid complex improved the antioxidant potential of gallic acid by enhancing its bioavailability. AAPS PharmSciTech. 2013;14(3):1025–33. https://doi.org/10.1208/s12249-013-9991-8.
39. Zeng B, Su M, Chen Q, Chang Q, Wang W, Li H. Antioxidant and hepatoprotective activities of polysaccharides from Anoectochilus roxburghii. Carbohydr Polym. 2016;153:391–8. https://doi.org/10.1016/j.carbpol.2016.07.067.
40. Chen Y, Miao Y, Huang L, Li J, Sun H, Zhao Y, et al. Antioxidant activities of saponins extracted from Radix Trichosanthis: an in vivo and in vitro evaluation. BMC Complement Altern Med. 2014;14. https://doi.org/10.1186/1472-6882-14-86.
41. Khan MR, Marium A, Shabbir M, Saeed N, Bokhari J. Antioxidant and hepatoprotective effects of Oxalis corniculata against carbon tetrachloride (CCl_4) induced injuries in rat. Afr J Pharm Pharmacol. 2012;6(30):2255–67. https://doi.org/10.5897/ajpp11.370.
42. Wu P, Ma G, Li N, Deng Q, Yin Y, Huang R. Investigation of in vitro and in vivo antioxidant activities of flavonoids rich extract from the berries of Rhodomyrtus tomentosa(Ait.) Hassk. Food Chem. 2015;173:194–202. https://doi.org/10.1016/j.foodchem.2014.10.023.
43. Yang Z, Wang J, Li J, Xiong L, Chen H, Liu X, et al. Antihyperlipidemic and hepatoprotective activities of polysaccharide fraction from Cyclocarya paliurus in high-fat emulsion-induced hyperlipidaemic mice. Carbohydr Polym. 2018;183:11–20. https://doi.org/10.1016/j.carbpol.2017.11.033.
44. Zhang QB, Li N, Zhou GF, Lu XL, Xu ZH, Li Z. In vivo antioxidant activity of polysaccharide fraction from Porphyra haitanesis (Rhodephyta) in aging mice. Pharmacol Res. 2003;48(2):151–5. https://doi.org/10.1016/s1043-6618(03)00103-8.
45. Li J-E, Nie S-P, Xie M-Y, Huang D-F, Wang Y-T, Li C. Chemical composition and antioxidant activities in immumosuppressed mice of polysaccharides isolated from Mosla chinensis Maxim cv. Jiangxiangru. Int Immunopharmacol. 2013;17(2):267–74. https://doi.org/10.1016/j.intimp.2013.05.033.
46. Gong YH, Wu YK, Zheng CL, Fan LY, Xiong F, Zhu JB. An excellent delivery system for improving the oral bioavailability of natural vitamin E in rats. AAPS PharmSciTech. 2012;13(3):961–6. https://doi.org/10.1208/s12249-012-9819-y.
47. El-Nahas AE, Allam AN, Abdelmonsif DA, El-Kamel AH. Silymarin-loaded Eudragit nanoparticles: formulation, characterization, and hepatoprotective and toxicity evaluation. AAPS PharmSciTech. 2017;18(8):3076–86. https://doi.org/10.1208/s12249-017-0799-9.